Journal of Power Sources 266 (2014) 393–400

Contents lists available at ScienceDirect

Journal of Power Sources

journal homepage: www.elsevier.com/locate/jpowsour

Densification of $Ce_{0.9}Gd_{0.1}O_{1.95}$ barrier layer by *in-situ* solid state reaction

De Wei Ni*, Vincenzo Esposito

Department of Energy Conversion and Storage, Technical University of Denmark, Frederiksborgvej 399, DK-4000 Roskilde, Denmark

HIGHLIGHTS

- Detailed understanding of the role of sintering aid under constrained condition.
- Densification of CGO barrier layer is achieved by *in-situ* solid state reaction.
- The *in-situ* solid state reaction technique can be extended to other multilayer system.

GRAPHICAL ABSTRACT

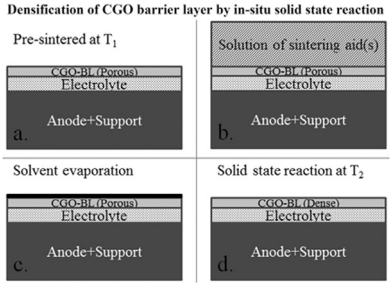

ARTICLE INFO

Article history:
Received 8 April 2014
Accepted 8 May 2014
Available online 21 May 2014

Keywords:
Sintering
CGO
SOFC
Multilayer ceramics

ABSTRACT

A novel methodology, called *in-situ* solid state reaction (SSR), is developed and achieved for the densification of gadolinia doped ceria (CGO) barrier layer (BL) within the solid oxide fuel cell (SOFC) technology. The method is based on the combined use of impregnation technique and a designed two-step sintering process to promote the densification of the CGO-BL on dense yttria stabilized zirconia (YSZ) electrolyte. A pre-sintering step is carried out at temperature T_1 (1150–1250 °C) to obtain porous and interconnected CGO-BL on dense electrolyte substrate. Impregnation of the porous BL is then carried out with small amount of either cobalt or copper nitrate solutions as sintering aids. Final sintering of the CGO-BL at temperature T_2 (1250–1275 °C, $T_2 > T_1$) is used to promote an SSR between the sintering aid and CGO-BL to obtain densification and grain growth. The approach proposed in this work was proved on both screen printed and tape cast CGO-BL, showing feasibility for the densification of generic ceramic multilayer systems undergoing different constrained sintering conditions and for a large variety of materials.

1. Introduction

The solid oxide fuel cell (SOFC) is a device that converts the chemical energy directly into heat and electricity. The SOFC is traditionally constructed from a strontium-substituted lanthanum manganite/yttria-stabilized zirconia (LSM/YSZ) cathode, a YSZ electrolyte, and a nickel/yttria-stabilized zirconia (Ni/YSZ) anode. To lower the operation temperature and reduce the cathode polarization of the SOFC, new cathode materials are developed. As an example, Fe–Co-based perovskites, *e.g.* (La,Sr)(Co,Fe)O_3 (LSCF) perform much better than the traditional LSM/YSZ cathodes [1]. However, these types of cathodes can react with the zirconia-based electrolyte forming $La_2Zr_2O_7$ and $SrZrO_3$ at high temperature [2,3]. The oxide-ion conductivity of $La_2Zr_2O_7$ and $SrZrO_3$ are 3.7×10^{-6} and 4.3×10^{-5} S cm^{-1} at 750 °C, respectively [4], which is much lower compared with the conductivity of pure YSZ (approximately

* Corresponding author. Tel.: +45 4677 5778; fax: +45 4677 5858.
E-mail addresses: dwei@dtu.dk, deweini2013@gmail.com (D.W. Ni).

http://dx.doi.org/10.1016/j.jpowsour.2014.05.044
0378-7753/

0.01 S cm^{-1}) [5]. The formation of these reaction products increases the ohmic polarization reducing significantly the cell performances. One solution to this issue is to employ a dense inter-diffusion barrier layer (BL) between the cathode and electrolyte to prevent the unfavorable chemical reaction. Usually, 10 mol% gadolinia doped ceria ($Ce_{0.9}Gd_{0.1}O_{1.95}$, CGO) is used as the barrier layer in this structure due to its high oxide ion conductivity, inertness towards LSCF, as well as chemical stability under cell operating conditions. And it has been shown that a dense CGO-BL can prevent the formation of a reaction layer between a Fe–Co-based cathode (*i.e.* LSCF) and a zirconia-based electrolyte [6,7].

To fabricate a CGO-BL, generally, a support is provided by conventional casting techniques, and on which an anode layer is formed at the green stage, *i.e.* non-sintered state, followed by the application of an electrolyte layer and/or a barrier layer in their respective green states, for example by multi casting techniques. The so-formed half-cell (HC) is dried and afterwards co-fired. In some cases, the CGO-BL is also deposited onto the pre-sintered HC in a separated processing step by different deposition techniques, such as screen printing, spray-coating, *etc.* and sintered. In the processing, selection of the sintering temperature is critical and aimed at obtaining an optimized configuration of the multilayer system, where the electrolyte and CGO-BL are dense, while the support and electrode layers are kept porous. However, the full densification of a CGO layer can be difficult due to the severe solute drag mechanism, which occurs in highly doped ceria [8–10]. Particularly, solute drag reduces elemental diffusion at the grain boundaries and limits grain growth and densification. Use of high temperatures can lead to excessive densification of the electrodes and detrimental ZrO_2–CeO_2 solid state reactions between the components at the interface [11]. Conversely, low sintering temperatures do not allow the desired air tightness by full densification of electrolyte and also the resulting CGO-BL can be porous. Consequently, the ohmic resistance of the cell may increase, and the CGO-BL properties towards the chemical reactivity of the layers may be lost. Moreover, different sintering activity of the layers in the multilayered system can lead to a constrained sintering process [12–16], which makes the densification of CGO-BL become difficult and complex.

Small amounts of sintering aids (mainly the transition metal oxides), such as NiO, Mn_2O_3, Co_2O_3, Co_3O_4, Fe_2O_3, and others can be added to CGO to enhance its densification [17–24]. The much preferred sintering aid in sintering of CGO is cobalt, either as oxides or as salts. Cobalt oxide is highly diffusive at high temperature and scarcely soluble in CGO. Moreover, it is an electric conductor which does not impair the electrical properties of CGO in low concentrations. Salts, *e.g.* cobalt nitrate, can liquefy, decompose and oxidize into cobalt oxide during the firing process. A significant lowering of the sintering temperature to about 950 °C in free sintering conditions of nano-metric CGO ceramics with addition of cobalt oxide has been reported by Kleinogel and Gauckler [17].

When sintering aids are used, they are usually mixed with the starting ceramic powders or used as a coating on the powders. However, although sintering aids enhance the sintering and densification of bulk materials in free sintering conditions, the effectiveness of such techniques has to be demonstrated as regards the formation of a dense thin ceramic layer (*i.e.* CGO-BL) in a multilayer system. The stress generated during the processing of the multilayer system can induce phenomena of creep or constrained sintering. Ceramic powders which are simply mixed with or covered by a sintering aid can thus be subject to severe viscous flow at high temperatures, among the particles and at the grain boundaries, leading to poorly sintered layers with formation of porosity or other defects during processes at high temperatures. The present work is dedicated to the investigation of the role of sintering aids, such as cobalt oxide, on the densification of CGO-BL in multilayered system under constrained condition. Moreover, an alternative methodology is proposed to introduce sintering aid into porous CGO-BL when it is needed, with an additional integrated *in-situ* solid state reaction (SSR) processing step. The outcome obtained in this work is also expected to be useful in other multilayered system, particularly the densification of top-layers which present limitations in terms of densification because of constrained sintering conditions, high sintering temperatures compared to the other layers, *etc.*

2. Experimental procedures

In this work, identical half cells consisting of a Ni/YSZ support, a Ni/YSZ fuel electrode and a YSZ electrolyte were used, which were fabricated by a standard procedure as described in Refs. [25,26]. The CGO-BL ($Ce_{0.9}Gd_{0.1}O_{1.95}$, specific surface area: 5.2 m^2 g^{-1}, Rhodia S.A., France) was deposited on top of the half-cell (HC), *i.e.* electrolyte, by screen printing technique (Scr-Print.) or by multi tape casting (MTC) [25,26]. The HC samples to be screen printed were sintered previously using a standard SOFC sintering procedure (here not reported) at the maximum temperature of 1250 °C. While for the MTC technique, the CGO-BL was deposited on green HC samples.

The densification of CGO-BL was carried out by an *in-situ* solid state reaction (SSR) technique. Schematic representation of the steps required in the procedure is illustrated in Fig. 1. Sintered half cells with porous CGO-BL are obtained at T_1 (Fig. 1a) as pre-sintered materials. The BL is thus impregnated by alcoholic solution of metal nitrate sintering aid(s) (Fig. 1b) and the solvent (ethanol) is then evaporated to allow an intimate precipitation of the aid into the porous BL network (Fig. 1c). In this work, $Co(NO_3)_2 \cdot 6H_2O$ or $Cu(NO_3)_2 \cdot 3H_2O$ (Sigma–Aldrich 99.999% trace metal basis) were used as sintering aid. The degree of the impregnation of the presented CGO-BL depends both on the concentration of the solution and the open porosity of the presented layer. Roughly, the amount of sintering aid can be estimated by assuming all the pores in the pre-sintered CGO-BL are filled with the solution of sintering aid after impregnation. Alternatively, the amount of sintering aid can also be determined by weighting the sample before and after the impregnation. In this work, the porosity of CGO-BL after pre-sintering was around 20–25%, and about 0.6–0.8 mol% sintering aid could be impregnated when sintering aid solution with 1 M concentration was used. Since excess of solution was always used in the impregnation step, precipitation of salt was observed at the surface of the HC. The impregnated material is successively treated at higher temperature T_2 ($T_2 > T_1$) where the SSR between CGO and cobalt oxide occurs (Fig. 1d). Temperature T_2 is designed to lead to densification of CGO-BL by SSR and it is selected as a function of T_1 and indeed on the diffusive and reactive features of the sintering aid. In this work, the temperatures of T_1 and T_2 were located in the range of 1150–1250 °C and 1250–1275 °C respectively. The heating rate after binder burnout is kept constant at 1 °C min^{-1} for all the treatment. All the samples used in the impregnation tests were small scale 2 × 2 cm obtained by cutting (diamond tip) and fracturing squared pieces from the starting large samples (16 × 16 cm and 5 × 5 cm samples). Due to the similar sample geometries, the stress–strain conditions generated during the co-firing are substantially equal for all the HC samples sintered at the same conditions.

The experiments were also accompanied by reference CGO-BL samples, where 2 mol% Co_3O_4 was mixed at the starting powders as sintering aids. The references underwent to the same thermal treatments used in the other SSR samples but without impregnation of sintering aids after pre-sintering at T_1. This was done to have a direct comparison on the microstructural evolution of the CGO-BLs with the action of sintering aid. All the HC samples used in this work had the same thickness of the anode support and comparable thickness of the electrolyte. The thickness of the CGO-BL

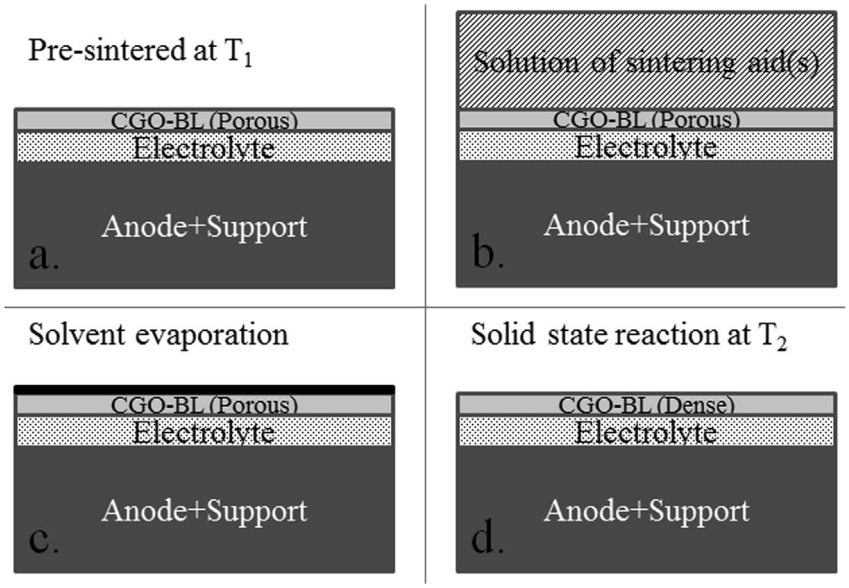

Fig. 1. Schematic description of the processing steps used in the densification of CGO-BL by *in-situ* SSR method.

ranged in the 3–10 μm depending on the deposition technique and the starting powders composition.

The linear shrinkage of the individual CGO-BL tape with 2 mol% Co_3O_4, HC (MTC sample, including BL) and pre-sintered HC in the in-plane direction during heat treatment was determined as a function of temperature by an optical dilatometer (TOMMI, Fraunhofer ISC, Würzburg, Germany). Green tape was tight rolled and pressed to obtain "bulky" sample of the thin layer which allowed dilatometry measurement. Details of the method are reported in our previous work [9,14–16]. This allows following samples shape evolution during sintering by *in-situ* and non-contact, simply collecting the sequent images of the samples' silhouettes projected by a source of visible light onto a high definition camera [10,27]. A "Non-contact" measurement is critical for the tape casting sample due to its intrinsic poor mechanical properties before sintering. The complete thermal cycle including de-binding step and sintering, was performed directly in the optical dilatometer to avoid moving the samples with possible mechanical failure after the de-binding step. Standard de-binding cycle included a slow heating ramp at 0.25 °C min^{-1} step from room temperature to 600 °C, and an isothermal treatment step at 600 °C for 4 h to ensure the binders removal. After binder burnout, the samples were then heated to 1300 °C at a constant heating rate of 1 °C min^{-1}.

The morphology of CGO-BL cross sections and top surfaces was examined using scanning electron microscopy (SEM). Low resolution imaging was performed using a Hitachi TM-1000, and a Carl Zeiss SUPRA along with energy dispersive X-ray spectroscopy (EDS) microanalysis detector was used for high resolution imaging and chemical analyses of the samples. SEM images of the material treated under different conditions were elaborated by ImageJ® freeware [28] to determine porosity fractions and other geometrical features.

3. Results and discussion

3.1. Sintering of CGO-BL with cobalt oxide mixed at the starting powders

3.1.1. Comparative analysis of individual component shrinkage during heat treatment: CGO-BL, HC and pre-sintered HC

A comparative analysis of shrinkage of individual component with HC during heat treatment was carried out under identical conditions to evaluate the critical stress in the multilayer system developed during sintering of the layers.

Fig. 2 shows the variations of shrinkage and corresponding shrinkage rate of free-standing rolled tape (no support) of the CGO-BL (with 2 mol% Co_3O_4 mixed at the starting powders), HC (MTC rolled tape sample, including BL) and pre-sintered rolled HC as a function of temperature, measured by monitoring the shape evolution at TOMMI dilatometer during heat treatment. The shrinkage determined from the de-binding (*i.e.*, the starting shrinkage before sintering) is not shown. Fig. 2a shows a continuous densification for both the CGO-BL and HC samples. With the addition of 2 mol% Co_3O_4 as sintering aid, the densification of the free-standing CGO-BL is activated at a very low temperature. It starts to shrink at around 750 °C and rapid shrinkage at 850–1000 °C is followed with a typical plateau of the final stage of sintering at around 1100 °C. In the main densification process within the temperature range of 750–1100 °C, the total shrinkage of CGO-BL is around 45%. This is consistent with other results reported for bulk CGO with cobalt oxide as sintering aid [17,20–22]. On the other hand, the half-cell (HC) shows very different densification behaviour. The data of HC in Fig. 2a illustrates the overall linear shrinkage behaviour of the rolled MTC sample composed of YSZ electrolyte and CGO-BL (to be dense) and Ni/YSZ support layers (to be porous) along the lateral direction. This represents the simultaneous contraction of all the layers in the in-plane directions. Fig. 2a shows that the HC sample starts to shrink at around 900 °C and continuous shrinkage is followed as temperature increase without the typical plateau of the final stage of sintering. The total shrinkage of HC is less than 20% in the whole sintering process indicating a constrained sintering condition of the single layers due to the reduced densification of the porous layers. Such conditions usually lead to the densification of electrolyte in the SOFC multilayer; however the multilayer is also accompanied by severe cambering and shape distortion effects (not discussed here), which is usually observed during the sintering multilayer system with an asymmetric distribution of the materials in the individual layers [12–16]. Fig. 2b shows a direct comparison of the shrinkage rate of CGO-BL and HC samples. The CGO-BL shrinks much faster than HC at temperatures below 1095 °C at the given heating rate; however, it becomes slower at higher temperatures. The CGO-BL achieves its highest shrinkage rate at about 980 °C, while HC at 1230 °C. It can be found that the main

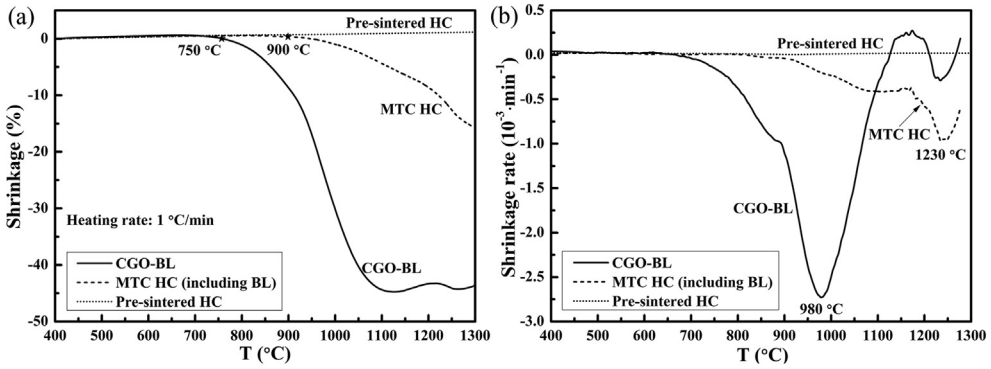

Fig. 2. Shrinkage and shrinkage rate of CGO-BL (with 2 mol% Co_3O_4 mixed at the starting powders), MTC HC (including CGO-BL) and pre-sintered HC as function of temperature during heat treatment at a heating rate of 1 °C min^{-1}.

deviation of the shrinkage rate between CGO-BL and HC locates in the temperature range of 800–1200 °C, which can result in serious constrained sintering when sintering the CGO-BL/HC multilayers. On the other hand, for the pre-sintered HC, no shrinkage is observed during heat treatment except limited thermal expansion. In conclusion, serious constrained stress can be expected during sintering the CGO-BL/HC multilayered structure, either in the MTC or Scr-Print system.

3.1.2. Microstructures of the sintered CGO-BL with cobalt oxide mixed at the starting powders

It is indicated from the TOMMI measurement (Fig. 2) that individual CGO-BL with Co_3O_4 mixed at the starting powders can be completely densified at temperatures higher than 1100 °C in free sintering. Fig. 3 shows the microstructures of the CGO-BLs co-fired on HC at 1275 °C/3 h. To make the thermal treatment more comparable with those CGO-BL sintered by *in-situ* SSR (reported in Section 3.2), a pre-sintering step at 1250 °C/5 h was carried out before sintering at 1275 °C/3 h. The microstructure of MTC CGO-BL without sintering aid is also shown here for comparison. From the SEM observations it can be found that the CGO-BL attached firmly to the HC. No cracks were found at the CGO-BL/HC interface or inside the CGO-BLs. A comparison between Fig. 3a and b clearly shows that the addition of cobalt oxide actually promotes the densification of CGO-BL, but the effect is very limited when the sintering aid is mixed at the starting powders. There is still a large fraction of mainly closed porosity uniformly spread on the top surface and cross section in the MTC CGO-BL. The case becomes even worse in the Scr-Print CGO-BL (Fig. 3d), indicating that the thermal expansion of the pre-sintered HC can induce formation of spread open porosity due to the detrimental stress conditions during the heat treatment. Particularly, presence of tensile stress during densification can easily reduce the sintering potential and separate the particles, especially when high diffusive sintering aid is present. Further evidences of such effect are revealed by SEM image analysis, which indicated that the porosity of CGO-BLs is around 20% and 30% respectively in the MTC and Scr-Print multilayered cell system (Fig. 3c and d). Moreover, the grain size of CGO is as small as around 0.5 μm after sintering at 1275 °C/3 h in the MTC system, which is about 0.3 μm in the Scr-Print system.

Compared with cerium, the diffusion coefficient of cobalt in oxide is 5–6 orders higher with much lower thermal activation energy [29], which is the original reason that cobalt addition can effectively promote the densification and grain growth of ceria. As an example, the diffusion coefficient D_{Co} in CoO is approximately 10^{-8} cm^2 s^{-1} at 1200 °C, whereas *e.g.* D_{Zr} in Ca-doped ZrO_2 (comparable to D_{Ce} in ceria) is approximately 10^{-14} cm^2 s^{-1} at 1200 °C. However, SEM images of the CGO-BLs show that very limited grain growth is detected in the layers (Fig. 3c and d). This is not consistent with other results obtained in free sintering condition for the cobalt oxide doped ceria [17,20–22]. This further observation clearly indicated that the cobalt failed to promote the mass diffusion of

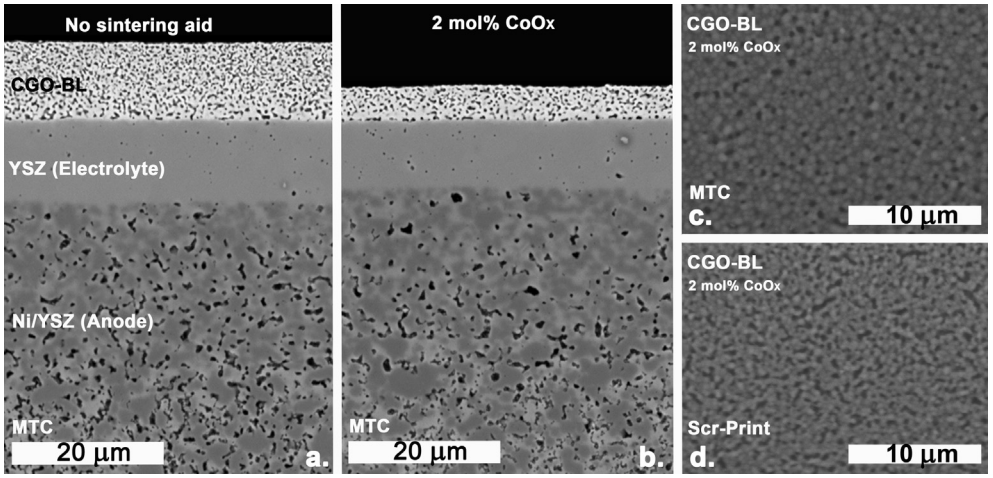

Fig. 3. Microstructures of CGO-BLs with/without cobalt oxide mixed at the starting powders after sintering at 1275 °C/3 h: (a) cross section of MTC CGO-BL without sintering aid; (b) cross section of MTC CGO-BL with 2 mol% cobalt oxide; (c) top surface of MTC CGO-BL with 2 mol% cobalt oxide; (d) top surface of Scr-Print CGO-BL with 2 mol% cobalt oxide.

CGO in the multilayered cell system. The unusual densification and grain growth behaviour in CGO-BL can be due to the effect of stress (and strain) induced by constrained sintering. A comparison of the shrinkage of individual CGO-BL, HC and pre-sintered HC samples in Fig. 2, treated under the same conditions, indicates a severe constrained sintering condition in the CGO-BL/HC multilayered system. The densification (shrinkage) of the cobalt oxide doped CGO-BL is fully activated at temperatures around 750 °C in free sintering, while the shrinkage in HC or pre-sintered HC is negligible below 1000 °C. This imposed a remarkable tensile stress in the CGO-BL during co-firing. The CGO powders which are simply mixed with cobalt oxide sintering aid is subject to severe viscous flow among the particles and at the grain boundaries, leading to poorly sintered CGO-BLs with formation of porosity during processes at high temperatures. The tensile stress becomes more serious when CGO-BL is co-fired on pre-sintered HC, leading to poorer densification and grain growth in the Scr-Print system (Fig. 3d). It can be expected the imposed tensile stress in the investigated status is comparable or even larger than general sintering stress (compression stress), which is in the range of 1–2 MPa [15,30].

3.2. Densification of CGO-BL by in-situ solid state reaction (SSR)

Due to the tensile stress generated during the processing of the multilayered system, it is ineffective to form a dense CGO-BL, when sintering aid is mixed with the starting ceramic powders. These problems are expected to be overcome by employing an alternative methodology, where the sintering aids are introduced into porous CGO-BL "when it is needed", by an additional integrated *in-situ* solid state reaction (SSR) processing step. This novel technique is based on the combined use of impregnation technique of sintering aid compounds into the CGO-BL and designed thermal treatments to promote its densification. The thermal treatments used in the sintering procedures include an intermediate step at room temperature allowing the impregnation of sintering aid compounds into the pre-sintered porous CGO-BL (see also Fig. 1). The pre-sintering step is carried out at a temperature T_1 which is carefully selected to obtain porous but interconnected CGO-BL on the dense electrolyte and robust cell. Since the densification is mainly based on grain boundary and lattice diffusion mechanisms [8], it is crucial at this step to ensure a proper connection and necking between the CGO particles. Impregnation of the porous BL is carried out with cobalt or copper nitrate solution as sintering aid. Final sintering and densification of the BL is the last firing procedure at temperatures T_2 ($T_2 > T_1$) used to promote an SSR between the sintering aid and the polycrystalline CGO layer. It is important to note that at such a stage, already connected and consolidated CGO in the first step, reacts actively at higher temperatures with cobalt regenerating the condition for further mass diffusion. In such conditions the grain boundary and lattice mechanisms become dominant again, leading to densification and grain growth.

3.2.1. Typical microstructures of CGO-BL densified by in-situ solid state reaction (SSR)

Fig. 4 shows the microstructures of CGO-BLs on half cells pre-sintered at 1250 °C/5 h (T_1) and densified by *in-situ* solid state reaction (SSR) at 1275 °C/3 h (T_2). The results of CGO-BLs prepared both by MTC and Scr-Print are presented together for comparison. After pre-sintering at 1250 °C/5 h (Fig. 4a and b), the CGO-BLs show a very porous structure, especially for the Scr-Print system. However, remarkable particle necking could be observed, indicating that a significant sintering occurred at 1250 °C. As pointed out, this is considered very important to ensure the porous body is strong enough for the next impregnation step. It should be noted that no sintering aid was used at this stage. But use of a small amount of sintering aid in the starting powders could also be considered if the particle necking is too limited at the processing temperature. Image analysis indicated that the porosity of CGO-BLs is around 20–25% with no grain growth in both cases of MTC and Scr-Print. The microstructure characteristics are comparable to the CGO-BLs with cobalt oxide sintering aid mixed at the starting powders, sintered at 1275 °C/3 h, as shown in Fig. 3c and d. This indicates again that it is ineffective to densify the CGO-BL when cobalt oxide sintering aid is mixed at the starting ceramic powders.

After pre-sintering, cobalt nitrate solution with 1 M concentration is impregnated directly into the porous CGO-BLs as sintering aid. The solvent (ethanol) is then evaporated to allow an intimate precipitation of the cobalt nitrate into the porous CGO-BL network. The impregnated material is successively sintered at 1275 °C/3 h. During this process, the cobalt nitrate is decomposed into cobalt oxide, and the SSR between CGO and cobalt oxide occurs. As shown in Fig. 4c and e, nearly dense CGO-BL is obtained

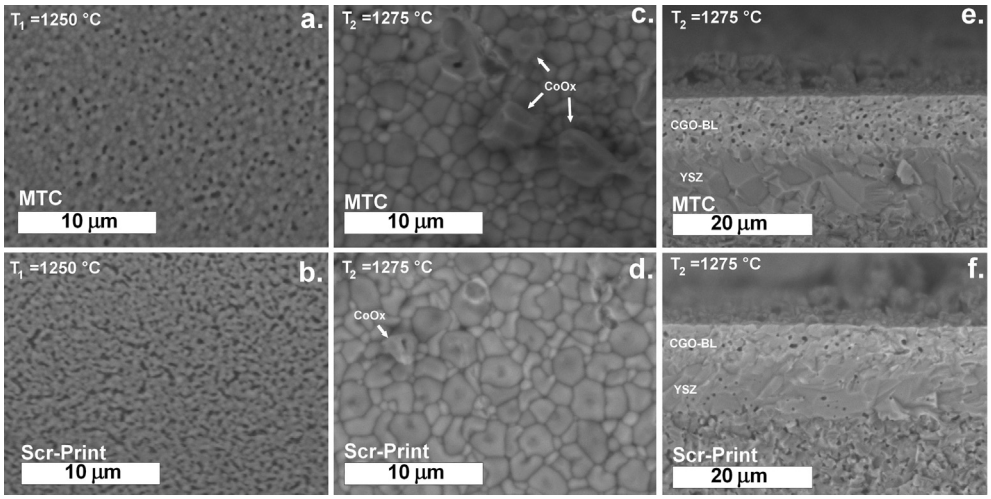

Fig. 4. Microstructures of CGO-BLs pre-sintered at 1250 °C/5 h (T_1) and densified by *in-situ* solid state reaction (SSR) at 1275 °C/3 h (T_2), using 1 M cobalt nitrate for impregnation: (a) top surface of MTC CGO-BL pre-sintered at 1250 °C/5 h (T_1); (b) top surface of Scr-Print CGO-BL pre-sintered at 1250 °C/5 h (T_1); (c) top surface of MTC CGO-BL densified by SSR at 1275 °C/3 h (T_2); (d) top surface of Scr-Print CGO-BL densified by SSR at 1275 °C/3 h (T_2); (e) cross section of MTC CGO-BL densified by SSR at 1275 °C/3 h (T_2); (f) cross section of Scr-Print CGO-BL densified by SSR at 1275 °C/3 h (T_2).

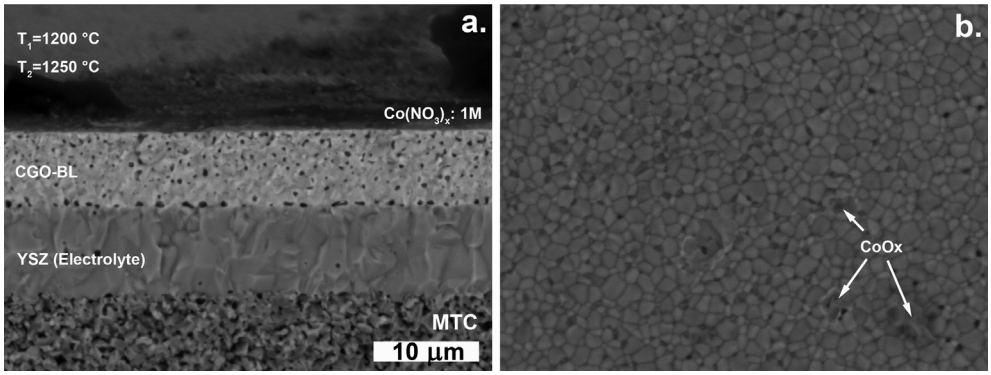

Fig. 5. Microstructures of MTC CGO-BL pre-sintered at 1200 °C/5 h (T_1) and densified by SSR at 1250 °C/3 h (T_2), using 1 M cobalt nitrate for impregnation: (a) cross section; (b) top surface.

in the MTC multilayered cell system. After sintering at 1275 °C/3 h with *in-situ* SSR, the porosity is determined less than 5%, by image analysis on Fig. 4c. While, the CGO-BL in Scr-Print system is fully densified (Fig. 4d and f). Moreover, the grain size in the CGO-BLs is as large as 2 μm, indicating remarkable grain growth happened during the SSR process. Figs. 3 and 4 show a direct comparison between the microstructures obtained for the CGO-BLs by identical thermal treatment but different chemical routes. It is clearly revealed that the diffusivity of the cobalt oxide sintering aid is activated simultaneously with the CGO-BLs during the SSR at 1275 °C (T_2). Moreover, as the CGO-BLs is first sintered and consolidated, particles are connected in the absence of, or with limited use of, sintering aids in the pre-sintering step (T_1). This allows for an effective action of the selected sintering aid over the sintering mechanism and the possibility of an optimized tailoring of the final microstructure in the ceramic layer, and contamination of the grain boundary is reduced.

3.2.2. Selection of T_1 and T_2 for the densification of CGO-BL by SSR

As reported in section 3.2.1, the pre-sintering temperature T_1 is selected so as to obtain dense electrolyte, fair mechanical strength, chemical properties required and to achieve the early particles necking with a certain degree of open porosity in the CGO-BL. However, such temperature depends on several parameters such as compositions of the materials used in the components, load, thickness of each layer, size of the cell, *etc*. As a consequence, to fully screen the feasibility of the method, several different T_1 were used in the experiment starting from a minimum of 1150 °C to a maximum of 1250 °C. The use of a thermal treatment at a temperature $T_2 > T_1$ is crucial to reactivate the sintering and grain growth mechanisms in the porous CGO-BL after having been pre-sintered at a temperature T_1. The diffusion and penetration of the sintering aid through the layer will depend on the initial porosity of the layer, time and temperatures used in the process. In this work, the maximum temperature T_2 for the SSR step was kept 25 °C above T_1, *i.e.* 1275 °C when 1250 °C was used as T_1, in way to allow densification avoiding large chemical modification of the materials. In other cases of T_1, the T_2 was fixed at 1250 °C.

The holding times used both in T_1 and T_2 treatments are selected starting from analysis of the sintering conditions. However, at this stage of the study the time is not considered as a critical parameter and different values can be chosen as function of the size of the sample, the furnace, *etc*. or to lead grain growth or sintering aid evaporation. In this work, the holding times were fixed at 5 h and 3 h respectively for T_1 and T_2.

As an example, Fig. 5 shows the microstructures of MTC CGO-BL pre-sintered at 1200 °C/5 h (T_1) and densified by *in-situ* solid state reaction (SSR) at 1250 °C/3 h (T_2). Fig. 5a shows the cross section of the sintered CGO-BL, and Fig. 5b shows the top surface structure. It can be found that a nearly dense barrier layer with enlarged grains is obtained under this temperature profile. Therefore, it shows a potential probability to decrease the densification temperature for CGO-BL, at a temperature slightly above the sintering temperature used in the cell fabrication. This is very beneficial to mitigate the stress during co-firing of the multilayered cell system. The decrease of sintering temperature is also helpful to avoid reactivity between CGO-BL and YSZ electrolyte.

3.2.3. Sintering aid and its influence on the microstructure of CGO-BL densification by SSR

Traces of sintering aids segregated at a high temperature (*i.e.* T_2) can usually be detected by EDS in the microstructure crystallized at the CGO-BL surface and/or trapped in the primary porosity and/or in the CGO-BL/HC interface, as pointed out by arrows in Figs. 4c,

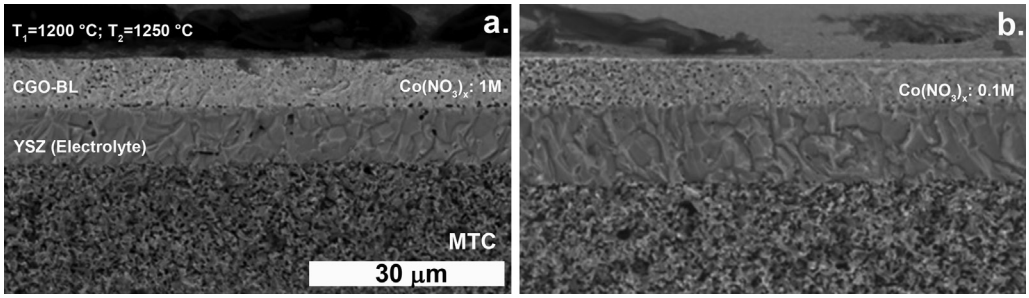

Fig. 6. Cross-sections of MTC CGO-BLs pre-sintered at 1200 °C/5 h (T_1) and densified by SSR at 1250 °C/3 h (T_2), but cobalt nitrate solutions with different concentrations were used for impregnation: (a) 1 M; (b) 0.1 M.

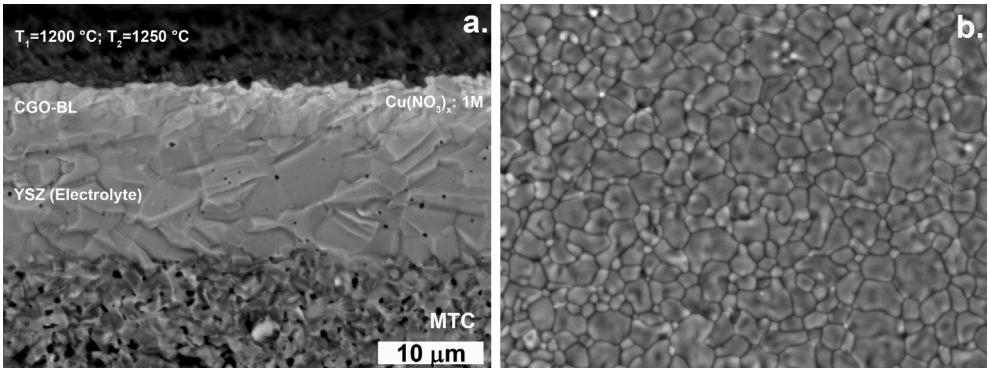

Fig. 7. Microstructures of MTC CGO-BL pre-sintered at 1200 °C/5 h (T_1) and densified by SSR at 1250 °C/3 h (T_2), using 1 M copper nitrate for impregnation: (a) cross section; (b) top surface.

d and 5b. However, such traces can be partially or completely removed from the layer surface by chemical etching or by additional treatments at the evaporation temperature(s) of the sintering aid(s). A selected chemical etching to remove the sintering aid(s) can also be used, if necessary and/or applicable, to clean the layer surface as a final step in the process.

Alternatively, the amount of cobalt sintering aid can be adjusted to reduce the contamination in the microstructure. As stated in the experimental part, the amount of sintering aid is partly dependent on the concentration of sintering aid solution used for impregnation. Fig. 6 shows a comparison of MTC CGO-BL pre-sintered at 1200 °C/5 h and densified by SSR at 1250 °C/3 h, but cobalt nitrate solutions with different concentrations were used for impregnation: 1 M and 0.1 M. When 0.1 M cobalt solution was used, its distribution in porous CGO-BL was not even, resulting in inhomogeneous densification of the CGO-BL, as shown in Fig. 6b. However, excess of cobalt oxide can be observed at the cross-section of the CGO-BL when 1 M cobalt solution was used (Fig. 6a). Thereby, an optimum concentration of cobalt solution used for impregnation might be between 0.1 M and 1 M.

Besides the most preferred cobalt oxides/salts, other sintering aids can also be used to impregnate into the CGO-BL, including Fe, Cr, Mn, Ni, Zn, Cu, Bi, Li, K, Ca or Ba salts and/or oxides and their mixtures. These sintering aids present a high diffusivity in the temperature range about 600–1400 °C [29] and electrical conductivity/catalytic properties under the operative conditions of SOFCs. As an example, Fig. 7 shows the microstructure of MTC CGO-BL pre-sintered at 1200 °C/5 h (T_1) and densified by SSR at 1250 °C/3 h (T_2), but 1 M copper nitrate solution was impregnated as sintering aid. Comparably to the microstructure of CGO-BL with 1 M cobalt nitrate shown in Figs. 5 and 6a, dense barrier layer with markedly enlarged grains is obtained when copper nitrate is used as sintering aid. This suggests that the SSR method can be applied with different sintering aids.

4. Summary and conclusions

In the development of high performance solid oxide fuel cell (SOFC), a dense gadolinia doped ceria (CGO) barrier layer (BL) between a Fe–Co-based cathode and a zirconia-based electrolyte can prevent the unfavorable reaction between them. Using conventional processing however, densification of CGO-BL is difficult to achieve due to constrained sintering condition. In this work, dense and crack free CGO-BL was successfully acquired on nickel/yttria stabilized zirconia (Ni/YSZ) anode supported half cells by a novel technique: *in-situ* solid state reaction (SSR). This technique is based on the combined use of impregnation technique of small amount of sintering aid compounds into pre-sintered CGO-BL and designed thermal treatments to promote its densification. At higher temperatures, pre-sintered porous CGO-BL reacts actively with cobalt/copper sintering aid, regenerating the condition for further mass diffusion and leading to the densification and grain growth of CGO-BL. The constrained sintering of CGO-BL within SOFC is overcome by using this novel technique processing, where densification and grain growth are enhanced.

The proposed approach in this work has mainly been developed for the densification of barrier layers of doped cerium oxide (*e.g.* gadolinia-doped cerium oxide) within SOFC technology. But it may also be used for the densification of ceramic multilayer systems in general. In fact the technology is compatible with the processing of many multilayer ceramic systems where the layer to be densified, can be impregnated by using sintering aids in solution or suspension. Furthermore, the densification of a given top layer during the preparation of a multilayer system can be followed by the deposition and densification of further porous layers. Therefore, the method can be applied to obtain a sequel of densified ceramic layers starting from a primary pre-sintered support.

Acknowledgement

The authors are grateful to Karen Brodersen, Søren P.V. Foghmoes and Johan Hjelm at DTU Energy Conversion, for supplying the stating materials used in this study.

References

[1] P. Plonczak, M. Joost, J. Hjelm, M. Søgaard, M. Lundberga, P.V. Hendriksen, J. Power Sources 196 (2011) 1156–1162.
[2] G.C. Kostogloudis, C. Ftikos, J. Eur. Ceram. Soc. 18 (1998) 1707–1710.
[3] S. Simner, J. Shelton, M. Anderson, J. Stevenson, Solid State Ionics 161 (2003) 11–18.
[4] F.W. Poulsen, N. Puil, Solid State Ionics 53–56 (1992) 777–783.
[5] T. Ishihara, N.M. Sammes, O. Yamamoto, High Temperature Solid Oxide Fuel Cells –Fundamentals, Design and Applications, Elsevier Ltd., Oxford, UK, 2003.
[6] L. Rose, M. Menon, K. Kammer, O. Kesler, P.H. Larsen, Adv. Mater. Res. 15–17 (2006) 293–298.
[7] K.K. Hansen, M. Menon, J. Knudsen, N. Bonanos, M. Mogensen, J. Electrochem. Soc. 157 (2010) B309–B313.
[8] P.L. Chen, I.W. Chen, J. Am. Ceram. Soc. 79 (1996) 1793–1800.
[9] D.W. Ni, C.G. Schmidt, F. Teocoli, A. Kaiser, K.B. Andersen, S. Ramousse, V. Esposito, J. Eur. Ceram. Soc. 33 (2013) 2529–2537.
[10] D.W. Ni, V. Esposito, S.P.V. Foghmoes, S. Ramousse, J. Eur. Ceram. Soc. 34 (2014) 2371–2379.
[11] A. Mai, V.A. Haanappel, F. Tietz, D. Stöver, Solid State Ionics 177 (2006) 2103–2107.
[12] J.D. Nicholas, L.C. DeJonghe, Mater. Res. Soc. Symp. Proc. 1023 (2007) 51–56.
[13] E. Olevsky, T.T. Molla, H.L. Frandsen, R. Bjøk, V. Esposito, D.W. Ni, A. Ilyina, N. Pryds, J. Am. Ceram. Soc. 96 (2013) 2657–2665.
[14] D.W. Ni, E. Olevsky, V. Esposito, T.T. Molla, S.P.V. Foghmoes, R. Bjøk, H.L. Frandsen, E. Aleksandrova, N. Pryds, J. Am. Ceram. Soc. 96 (2013) 2666–2673.

[15] D.W. Ni, V. Esposito, C.G. Schmidt, T.T. Molla, K.B. Andersen, A. Kaiser, S. Ramousse, N. Pryds, J. Am. Ceram. Soc. 96 (2013) 972–978.
[16] T.T. Molla, H.L. Frandsen, R. Bjørk, D.W. Ni, E. Olevsky, N. Pryds, J. Eur. Ceram. Soc. 33 (2013) 1297–1305.
[17] C. Kleinogel, L.J. Gauckler, Solid State Ionics 135 (2000) 567–573.
[18] M. Chen, B. Hallstedt, A.N. Grundy, L.J. Gauckler, J. Am. Ceram. Soc. 86 (2003) 1567–1570.
[19] T.S. Zhang, J. Ma, S.H. Chan, J.A. Kilner, J. Electrochem. Soc. 151 (2004) J84–J90.
[20] E. Jud, C.B. Huwiler, L.J. Gauckler, J. Am. Ceram. Soc. 88 (2005) 3013–3019.
[21] H. Yoshida, T. Inagaki, J. Alloys Compd. 408 (2006) 632–636.
[22] R. Yan, F. Chu, Q. Ma, X. Liu, G. Meng, Mater. Lett. 60 (2006) 3605–3609.
[23] J.D. Nicholas, L.C. DeJonghe, Solid State Ionics 178 (2007) 1187–1194.
[24] V. Esposito, M. Zunic, E. Traversa, Solid State Ionics 180 (2009) 1069–1075.
[25] A. Hagen, R. Barfod, P.V. Hendriksen, Y.L. Liu, S. Ramousse, J. Electrochem. Soc. 153 (2006) A1165–A1171.
[26] A. Hagen, M. Menon, R. Barfod, P.V. Hendriksen, S. Ramousse, P.H. Larsen, Fuel Cells 6 (2006) 146–150.
[27] F. Raether, J. Am. Ceram. Soc. 92 (2009) S146–S152.
[28] http://rsbweb.nih.gov/ij/.
[29] Y.M. Chiang, D. Birnie, W.D. Kingery, in: C. Robichaud, K. Santor (Eds.), Physical Ceramics: Principles for Ceramic Science and Engineering, John Wiley and Sons, New York, NY, 1996, p. 187.
[30] M. Chiang, J. Jean, S. Lin, Mater. Chem. Phys. 128 (2011) 413–417.